R-mode instability of strange stars and observations of neutron stars in LMXBs [*]

Chun-Mei Pi[1], Shu-Hua Yang[2] and Xiao-Ping Zheng[2]

[1] Department of Physics and Engineering, Hubei University of Education, Wuhan 430205, China
[2] Institute of Astrophysics, Central China Normal University, Wuhan 430079, China;
  ysh@phy.ccnu.edu.cn

Abstract   Using a realistic equation of state (EOS) of strange quark matter, namely, the modified bag model, and considering the constraints on the parameters of EOS by the observational mass limit of neutron stars, we investigate the r-mode instability window of strange stars, and find the same result as in the brief study of Haskell, Degenaar and Ho in 2012 that these instability windows are not consistent with the spin frequency and temperature observations of neutron stars in low mass X-ray binaries.

Key words: dense matter — stars: neutron — stars: oscillations

1 INTRODUCTION

The realization in 1998 that r-modes, which are restored by the Coriolis force, are subjected to Chandrasekhar-Friedmann-Schutz (CFS) instability (Chandrasekhar 1970; Friedman & Schutz 1978) in a perfect fluid star with arbitrary rotation (Andersson 1998; Friedman & Morsink 1998), has received a lot of attention. It is easy to understand that for a realistic neutron star, the r-mode instability only happens in a range of spin frequencies and temperatures, the so-called r-mode instability window, which is decided by the competition between the gravitational-wave driven effect and viscous-dissipation damping effect on the modes (Lindblom et al. 1998). Therefore, the r-mode instability is an important primary physical mechanism that can prevent neutron stars from spinning up to their Kepler frequency ($\Omega_{\rm K}$, above which matter is ejected from the star's equator) (Madsen 1998; Andersson et al. 1999), and gravitational waves emitted during the instability process could be detected (Andersson & Kokkotas 2001; Andersson et al. 2002; Abadie et al. 2010; Alford & Schwenzer 2014). In fact, some other aspects related to r-mode instability are also studied. For example, as an alternative explanation to the rapid cooling of the neutron star in Cas A (which can be well explained by the superfluidity-triggering model (Page et al. 2011; Shternin et al. 2011; Elshamouty et al. 2013)), it is suggested that the star experiences the recovery period following the r-mode heating process by assuming the star is differentially rotating (Yang et al. 2010, 2011).

Recently, as more and more temperature data on neutron stars in low mass X-ray binaries (LMXBs) have been presented through X-ray and UV observations (Haskell et al. 2012; Gusakov et al. 2014), many studies have tried to constrain the physics behind the r-mode instability of neutron stars, especially the equation of state (EOS) of cold dense matter, by comparing the r-mode

instability window with the spin frequency and temperature observations in these systems (Ho et al. 2011; Haskell et al. 2012; Vidaña 2012; Wen et al. 2012).

In this paper, we will investigate the case of strange stars in detail following the brief study by Haskell et al. (2012). Different from their work and other former works about r-modes in strange stars (e.g. Madsen 1998, 2000), our study is based on a realistic EOS of strange quark matter, namely, the modified bag model (Farhi & Jaffe 1984; Haensel et al. 1986; Alcock et al. 1986; Weber 2005). We give the timescales related to r-modes numerically; moreover, before our study of the r-mode instability window, we fix the parameter space of EOS so that it can match the mass limit of neutron stars, which is fixed by determining the mass of the millisecond pulsar PSR J1614-2230 to be $1.97 \pm 0.04\ M_\odot$ (Demorest et al. 2010), and has been further updated by the recent measurement of the $2.01 \pm 0.04\ M_\odot$ PSR J0348+0432 (Antoniadis et al. 2013).

Although strange stars can also support a thin crust of normal nuclear matter up to the neutron drip density (Glendenning & Weber 1992), it only leads to minor changes in the maximum mass compared with bare strange stars (Zdunik 2002), and it also does not contribute significantly to the damping of r-modes (Andersson et al. 2002; Haskell et al. 2012). Therefore, we only study the r-mode instability window of bare strange stars in this work, which will be very similar to strange stars with a nuclear crust. However, the r-mode instability window of strange stars with a crystalline superconducting quark crust will be very different, as studied by Rupak & Jaikumar (2013); we will not consider that case in this paper. Moreover, we will not consider the case of solid strange quark stars composed of quark clusters (Xu 2003; Yu & Xu 2011; Zhou et al. 2014), since apparently r-mode instability could not occur in these stars.

The plan of this paper is as follows. In Section 2, we briefly show the modified strange quark matter EOS used in our study, and calculate the allowed parameter space following certain constraints. In Section 3, we give the inequality through which the r-mode instability window is determined, and the related gravitational-wave driven timescale and the viscous-damping timescales are also presented. In Section 4, we compare the theoretical r-mode window with the spin frequency and temperature observations of neutron stars in LMXBs, and Section 5 is our conclusions and discussion.

2 EOS OF STRANGE QUARK MATTER AND CONSTRAINTS IMPOSED BY THE MASS OF PSR J1614-2230 AND PSR J0348+0432

For strange quark matter, we take the modified bag model (Farhi & Jaffe 1984; Haensel et al. 1986; Alcock et al. 1986; Weber 2005), in which up (u) and down (d) quarks are treated as massless particles while the strange (s) quark mass is a free parameter, and first-order perturbative corrections in the strong interaction coupling constant α_S are taken into account. The thermodynamic potentials for the u, d and s quarks, and for the electrons are (Alcock et al. 1986; Na et al. 2012)

$$\Omega_u = -\frac{\mu_u^4}{4\pi^2}\left(1 - \frac{2\alpha_S}{\pi}\right), \tag{1}$$

$$\Omega_d = -\frac{\mu_d^4}{4\pi^2}\left(1 - \frac{2\alpha_S}{\pi}\right), \tag{2}$$

$$\begin{aligned}
\Omega_s = -\frac{1}{4\pi^2}&\left\{\mu_s\sqrt{\mu_s^2 - m_s^2}\left(\mu_s^2 - \frac{5}{2}m_s^2\right) + \frac{3}{2}m_s^4 f(u_s, m_s)\right.\\
&-\frac{2\alpha_S}{\pi}\left[3\left(\mu_s\sqrt{\mu_s^2 - m_s^2} - m_s^2 f(u_s, m_s)\right)^2 - 2(\mu_s^2 - m_s^2)^2\right.\\
&\left.\left.-3m_s^4\ln^2\frac{m_s}{\mu_s} + 6\ln\frac{\sigma}{\mu_s}\left(\mu_s m_s^2\sqrt{\mu_s^2 - m_s^2} - m_s^4 f(u_s, m_s)\right)\right]\right\}, \tag{3}
\end{aligned}$$

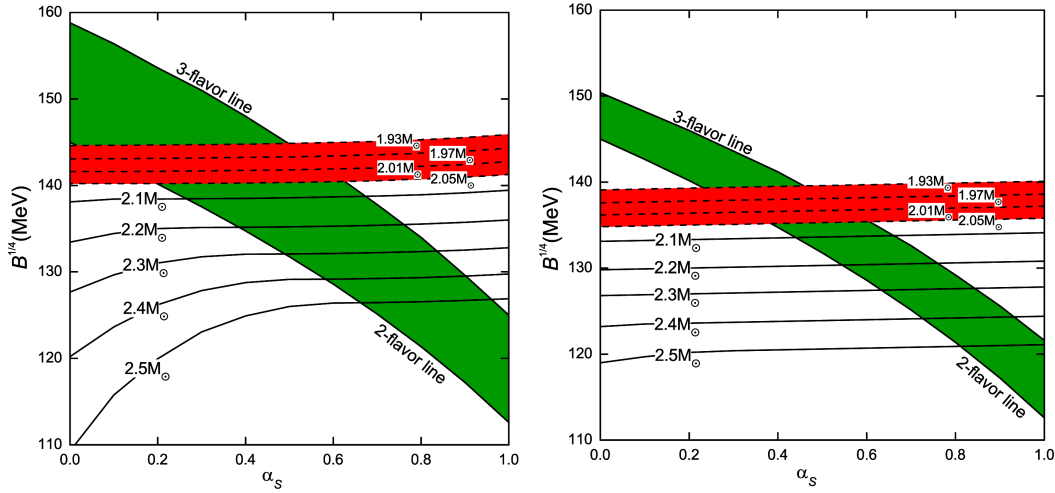$$\Omega_e = -\frac{\mu_e^4}{12\pi^2}, \tag{4}$$

Fig. 1 The constraints on the parameters of the EOS of strange quark matter, namely, $B^{1/4}$ and α_S. The green shaded area corresponds to the allowed parameter space according to the constraints of the absolute stability of strange quark matter (3-flavor line) and the existence of nuclei (2-flavor line). The red shaded area marks the parameter space which has the maximum mass of PSR J1614-2230 ($M = 1.97 \pm 0.04\ M_\odot$) and PSR J0348+0432 ($M = 2.01 \pm 0.04\ M_\odot$). The combinations of $B^{1/4}$ and α_S which could lead to the maximum mass of a strange star being $M = 2.1\ M_\odot$, 2.2 $M_\odot$, 2.3 $M_\odot$, 2.4 $M_\odot$, 2.5 $M_\odot$ are also presented. The two graphs are for $m_s = 100$ MeV (*left panel*) and $m_s = 200$ MeV (*right panel*), respectively.

where $f(u_s, m_s) \equiv \ln((\mu_s + \sqrt{\mu_s^2 - m_s^2})/m_s)$, σ is a renormalization constant whose value is of the order of the chemical potentials (Farhi & Jaffe 1984), and we take $\sigma = 300$ MeV in this paper. (Note, there is a typo in Na et al. 2012 before the term $3m_s^4 \ln^2 \frac{m_s}{\mu_s}$ for Ω_s, it should be "$-$" as given by Alcock et al. 1986.)

Before the discussion of the r-mode instability window of strange stars and making a comparison with observations of neutron stars in LMXBs, we calculate the allowed parameter space for the EOS of strange quark matter according to the following basic constraints (Schaab et al. 1997; Weissenborn et al. 2011; Wei & Zheng 2012). First, the existence of quark stars composed of stable strange quark matter is based on the idea that the presence of strange quarks can lower the energy per baryon of the mixture of u, d and s quarks in beta equilibrium below the one of ^{56}Fe ($E/A \sim 930$ MeV) (Witten 1984). This constraint results in the "3-flavor line" in Figure 1. The second constraint is given by the assumption that non-strange quark matter (two-flavor quark matter consists of only u and d quarks) in bulk has a binding energy per baryon higher than the one for the most stable atomic nucleus, ^{56}Fe, plus a 4 MeV correction coming from surface effects (Farhi & Jaffe 1984). By imposing that $E/A \geq 934$ MeV for non-strange quark matter, one ensures that atomic nuclei do not dissolve into their constituent quarks which leads to the "2-flavor line" in Figure 1. The last constraint is that the maximum mass must be greater than the masses of PSR J1614-2230 ($M = 1.97 \pm 0.04\ M_\odot$) and PSR J0348+0432 ($M = 2.01 \pm 0.04\ M_\odot$). This constraint can also be shown in Figure 1, since for each set of parameters of the strange quark matter EOS (namely, m_s, $B^{1/4}$ and α_S), one can derive a maximum mass by solving the Oppenheimer-Volkoff equations.

According to the above three constraints, the allowed parameter space is displayed in Figure 1. The region between the "3-flavor line" and "2-flavor line" (the green shaded area) is allowed according to the first two constraints, but considering the third constraint, only a part of the green shaded

area is allowed, namely, the part below the red shaded area. From Figure 1, it can be found that for our EOS model, both for the cases of $m_s = 100\,\mathrm{MeV}$ and $m_s = 200\,\mathrm{MeV}$, the constraint about the maximum mass results in $\alpha_S > 0$, which means the QCD corrections must be included, and it is the same result as given by Weissenborn et al. (2011).

3 R-MODE INSTABILITY WINDOW OF STRANGE STARS

The r-mode instability window of a strange star is defined by the inequality

$$\frac{1}{\tau_{\mathrm{GW}}} + \frac{1}{\tau_\eta} + \frac{1}{\tau_\zeta} < 0, \tag{5}$$

where τ_{GW} is the timescale of the growth of an r-mode due to the emission of gravitational waves; τ_η and τ_ζ are the dissipation timescales due to shear viscosity and bulk viscosity, respectively. For a strange star with given spin frequency Ω and core temperature T which satisfy the above inequality, the r-mode in the star should increase exponentially, and the amplified r-mode will transfer angular momentum of the star to gravitational waves; therefore, the star should quickly leave the instability window, making the probability of observing it in that region in the $\Omega - T$ plane (Gusakov et al. 2014) vanishingly small.

The growth timescale due to the emission of gravitational waves is given by Lindblom et al. (1998)

$$\frac{1}{\tau_{\mathrm{GW}}} = -\frac{32\pi G \Omega^{2l+2}}{c^{2l+3}} \frac{(l-1)^{2l}}{[(2l+1)!!]^2} \left(\frac{l+2}{l+1}\right)^{2l+2} \int_0^R \rho r^{2l+2} dr, \tag{6}$$

where Ω is the spin frequency of the star and ρ is the mass density in g cm^{-3}. In this paper, we only focus on the r-modes with quantum number $l = 2$ and azimuthal projection $m = 2$ because these are the dominant ones (Lindblom et al. 1998; Madsen 1998).

The dissipation timescale due to shear viscosity is (Lindblom et al. 1998)

$$\frac{1}{\tau_\eta} = (l-1)(2l+1) \left[\int_0^R \rho r^{2l+2} dr \right]^{-1} \int_0^R \eta r^{2l} dr. \tag{7}$$

The shear viscosity of strange quark matter due to quark scattering was calculated by Heiselberg & Pethick (1993), and the results for $T \ll \mu$, where T is the temperature and μ is the quark chemical potential, can be presented as (Madsen 1998)

$$\eta \approx 1.7 \times 10^{18} \left(\frac{0.1}{\alpha_S}\right)^{5/3} \rho_{15}^{14/9} T_9^{-5/3} \mathrm{g\,cm^{-1}\,s^{-1}}, \tag{8}$$

where $T_9 \equiv T/10^9\,\mathrm{K}$ and $\rho_{15} \equiv \rho/10^{15}\,\mathrm{g\,cm^{-3}}$.

The dissipation timescale due to bulk viscosity is given by references (Lindblom & Owen 2002; Nayyar & Owen 2006; Vidaña 2012). By considering second order effects (Lindblom et al. 1999)

$$\frac{1}{\tau_\zeta} = \frac{4\pi}{690} \left(\frac{\Omega^2}{\pi G \bar{\rho}}\right)^2 R^{2l-2} \left[\int_0^R \rho r^{2l+2} dr \right]^{-1} \int_0^R \zeta \left(\frac{r}{R}\right)^6 \left[1 + 0.86 \left(\frac{r}{R}\right)^2 \right] r^2 dr, \tag{9}$$

where $\bar{\rho} \equiv M/(4\pi R^3/3)$ is the average density of the nonrotating star. The bulk viscosity of strange quark matter mainly depends on the rate of non-leptonic weak interaction (Wang & Lu 1984; Sawyer 1989; Madsen 1992)

$$u + d \leftrightarrow s + u. \tag{10}$$

To a good approximation, the bulk viscosity is (Madsen 1992)

$$\zeta \approx \alpha T^2 / [\omega^2 + \beta T^4], \tag{11}$$

with α and β given by Madsen (1992), and ω is the angular frequency of the perturbation. During the study of r-mode instability, ω is the angular frequency of the r-mode perturbation $\omega_r = 2m\Omega/l(l+1)$, where Ω is the spin frequency of the star. For the dominant r-mode ($m = l = 2$), $\omega = \frac{2}{3}\Omega$. The low-$T$ limit ($T < 10^9$ K) is enough for this work, and it turns out to be (Madsen 2000)

$$\zeta \approx 3.2 \times 10^{28} m_{100}^4 \rho_{15} T_9^2 \omega^{-2} \mathrm{g\,cm^{-1}\,s^{-1}}\,, \tag{12}$$

where m_{100} is the strange quark mass in units of $100\,\mathrm{MeV}$ and all the other quantities are in cgs units.

4 COMPARING THE INSTABILITY WINDOW WITH OBSERVATIONS

By solving the inequality (5), together with Equations (6), (7) and (9) numerically for given parameter sets for the EOS of strange quark matter, one can derive the r-mode instability window for strange stars. Here, we want to stress that we will only discuss the parameter sets of the strange quark matter EOS which reside in the allowed parameter space as shown in Section 2.

Figure 2 shows the r-mode instability window for a strange star with the canonical neutron star mass $M = 1.4\,M_\odot$, and the observational data on the spin frequency and internal temperature of neutron stars in LMXBs, which are given by Gusakov et al. (2014). The left panel is for $m_s = 100\,\mathrm{MeV}$ and $B^{1/4} = 140\,\mathrm{MeV}$, and the right panel is for $m_s = 200\,\mathrm{MeV}$ and $B^{1/4} = 135\,\mathrm{MeV}$. (For each given m_s, we select the largest approximate $B^{1/4}$ value that is allowed by the limit of observational neutron star mass according to Fig. 1, because it corresponds to a smaller allowed α_S, which will lead to a smaller r-mode instability region as can be seen in Fig. 2.) For the left panel, three curves are presented, which represent the cases of $\alpha_S = 0.2$, $\alpha_S = 0.4$ and $\alpha_S = 0.6$, respectively; while for the right panel, we only show two curves, namely $\alpha_S = 0.4$ and $\alpha_S = 0.6$.
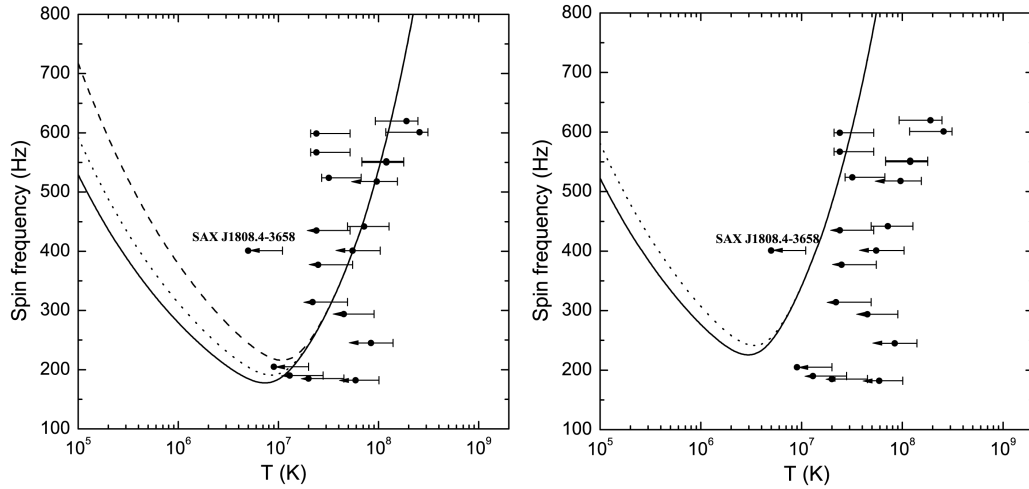

Fig. 2 R-mode instability window for a strange star with $M = 1.4\,M_\odot$, compared with the observational data on the spin frequency and internal temperature of neutron stars in LMXBs (Gusakov et al. 2014). The left panel is for $m_s = 100\,\mathrm{MeV}$ and $B^{1/4} = 140\,\mathrm{MeV}$, and the right panel is for $m_s = 200\,\mathrm{MeV}$ and $B^{1/4} = 135\,\mathrm{MeV}$. The dashed, dotted and solid curves correspond to $\alpha_S = 0.2$, $\alpha_S = 0.4$ and $\alpha_S = 0.6$, respectively. (Note, there is no dashed curve in the right panel because non-strange quark matter does not satisfy the condition $E/A \geq 934\,\mathrm{MeV}$ for the parameter set $\alpha_S = 0.2$, $m_s = 200\,\mathrm{MeV}$ and $B^{1/4} = 135\,\mathrm{MeV}$, which can be seen in Fig. 1.)
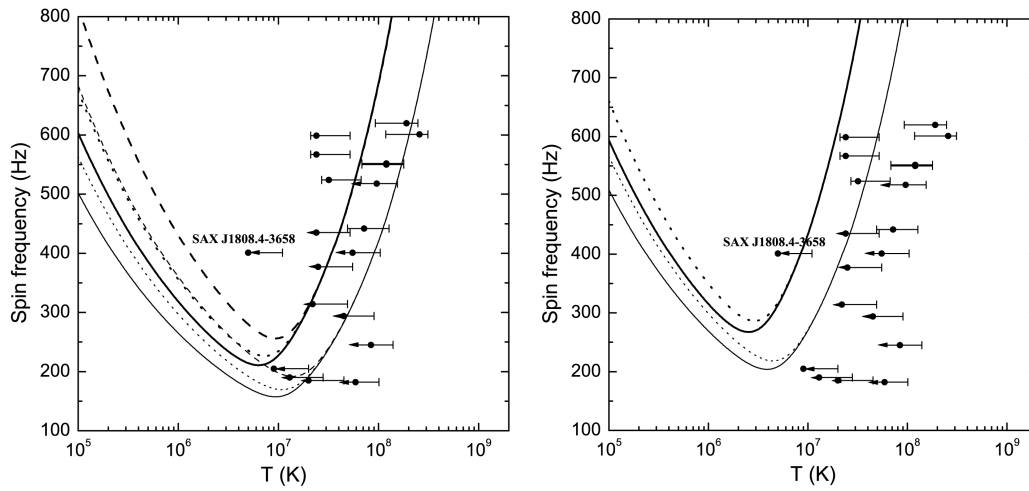
Fig. 3 Similar to Fig. 2, but for strange stars with $M = 1.0\ M_\odot$ (*thick lines*) and $M = 2.0\ M_\odot$ (*thin lines*).

The reason is that the parameter set $\alpha_S = 0.2$, $m_s = 200\ \text{MeV}$ and $B^{1/4} = 135\ \text{MeV}$ is not located in the allowed parameter space as discussed in Section 2; more exactly, non-strange quark matter does not satisfy the condition $E/A \geq 934\ \text{MeV}$ for this parameter set. It can be seen that all the possible instability windows are not consistent with the spin frequency and temperature observations of neutron stars in LMXBs, which turns out to be the same conclusion as drawn by Haskell et al. (2012).

In Figure 3, we present the r-mode instability window for strange stars with $M = 1.0\ M_\odot$ and $M = 2.0\ M_\odot$. From this graph, one can draw the same conclusion as stated above from Figure 2. However, as one can see from the thick curves in the right panel of Figure 3, for fixed parameter set $M = 1.0\ M_\odot$, $m_s = 200\ \text{MeV}$ and $B^{1/4} = 135\ \text{MeV}$, both of the two curves (for $\alpha_S = 0.4$ and $\alpha_S = 0.6$, respectively) can explain well all the observational data except the data point representing SAX J1808.4–3658. Therefore, the source SAX J1808.4–3658 is very important for us to consider when drawing any conclusions.

5 CONCLUSIONS AND DISCUSSION

Following the brief study by Haskell et al. (2012), we examine the instability window of strange stars in detail, and compare it with the spin frequency and temperature observations of neutron stars in LMXBs. Our work is based on a realistic EOS of strange quark matter, namely, the modified bag model. Besides the numerical calculation of the timescales related to r-modes, we also employ a delicate strategy, in which firstly, we calculate the allowed parameter space of EOS so that it can match the observed mass limit of neutron stars, and then the study of the instability window of strange stars and its comparison with the observations are carried out.

Our study confirms the conclusion given by Haskell et al. (2012) that all the possible instability windows of strange stars are not consistent with the spin frequency and temperature observations of neutron stars in LMXBs. However in this paper, as far as the bulk viscosity of strange quark matter is concerned, it is calculated under the non-interacting Fermi liquid model (Madsen 1992). If the interactions which lead to non-Fermi liquid effects are included, the bulk viscosity ζ can be increased by many orders of magnitude (Zheng et al. 2002, 2003, 2005; Schwenzer 2012), and the
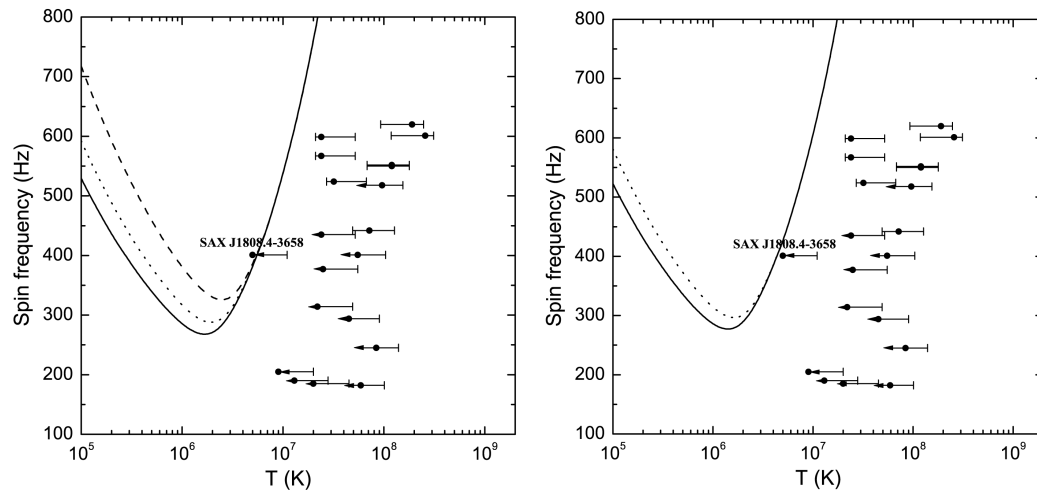
Fig. 4 Similar to Fig. 2, but ζ is artificially taken to be 100 times larger in the left panel and 10 times larger in the right panel.

instability window may be consistent with the observations. This possibility is shown roughly in Figure 4, using the same parameter sets of EOS as Figure 2 but the bulk viscosity ζ is artificially taken to be 100 times larger in the left panel and 10 times larger in the right panel. It can be seen from Figure 4 that the instability window could almost be consistent with observations under the above assumptions. A detailed study about that possibility will be carried out in our future work.

References

Abadie, J., Abbott, B. P., Abbott, R., et al. 2010, ApJ, 722, 1504

Alcock, C., Farhi, E., & Olinto, A. 1986, ApJ, 310, 261

Alford, M. G., & Schwenzer, K. 2014, ApJ, 781, 26

Andersson, N. 1998, ApJ, 502, 708

Andersson, N., Kokkotas, K. D., & Stergioulas, N. 1999, ApJ, 516, 307

Andersson, N., & Kokkotas, K. D. 2001, International Journal of Modern Physics D, 10, 381

Andersson, N., Jones, D. I., & Kokkotas, K. D. 2002, MNRAS, 337, 1224

Antoniadis, J., Freire, P. C. C., Wex, N., et al. 2013, Science, 340, 448

Chandrasekhar, S. 1970, ApJ, 161, 561

Demorest, P. B., Pennucci, T., Ransom, S. M., Roberts, M. S. E., & Hessels, J. W. T. 2010, Nature, 467, 1081

Elshamouty, K. G., Heinke, C. O., Sivakoff, G. R., et al. 2013, ApJ, 777, 22

Farhi, E., & Jaffe, R. L. 1984, Phys. Rev. D, 30, 2379

Friedman, J. L., & Schutz, B. F. 1978, ApJ, 221, 937

Friedman, J. L., & Morsink, S. M. 1998, ApJ, 502, 714

Glendenning, N. K., & Weber, F. 1992, ApJ, 400, 647

Gusakov, M. E., Chugunov, A. I., & Kantor, E. M. 2014, Physical Review Letters, 112, 151101

Haensel, P., Zdunik, J. L., & Schaefer, R. 1986, A&A, 160, 121

Haskell, B., Degenaar, N., & Ho, W. C. G. 2012, MNRAS, 424, 93

Heiselberg, H., & Pethick, C. J. 1993, Phys. Rev. D, 48, 2916

Ho, W. C. G., Andersson, N., & Haskell, B. 2011, Physical Review Letters, 107, 101101

Lindblom, L., Owen, B. J., & Morsink, S. M. 1998, Physical Review Letters, 80, 4843

Lindblom, L., Mendell, G., & Owen, B. J. 1999, Phys. Rev. D, 60, 064006

Lindblom, L., & Owen, B. J. 2002, Phys. Rev. D, 65, 063006

Madsen, J. 1992, Phys. Rev. D, 46, 3290

Madsen, J. 1998, Physical Review Letters, 81, 3311

Madsen, J. 2000, Physical Review Letters, 85, 10

Na, X., Xu, R., Weber, F., & Negreiros, R. 2012, Phys. Rev. D, 86, 123016

Nayyar, M., & Owen, B. J. 2006, Phys. Rev. D, 73, 084001

Page, D., Prakash, M., Lattimer, J. M., & Steiner, A. W. 2011, Physical Review Letters, 106, 081101

Rupak, G., & Jaikumar, P. 2013, Phys. Rev. C, 88, 065801

Sawyer, R. F. 1989, Physics Letters B, 233, 412

Schaab, C., Hermann, B., Weber, F., & Weigel, M. K. 1997, Journal of Physics G Nuclear Physics, 23, 2029

Schwenzer, K. 2012, arXiv:1212.5242

Shternin, P. S., Yakovlev, D. G., Heinke, C. O., Ho, W. C. G., & Patnaude, D. J. 2011, MNRAS, 412, L108

Vidaña, I. 2012, Phys. Rev. C, 85, 045808

Wang, Q. D., & Lu, T. 1984, Physics Letters B, 148, 211

Weber, F. 2005, Progress in Particle and Nuclear Physics, 54, 193

Wei, W., & Zheng, X.-P. 2012, Astroparticle Physics, 37, 1

Weissenborn, S., Sagert, I., Pagliara, G., Hempel, M., & Schaffner-Bielich, J. 2011, ApJ, 740, L14

Wen, D.-H., Newton, W. G., & Li, B.-A. 2012, Phys. Rev. C, 85, 025801

Witten, E. 1984, Phys. Rev. D, 30, 272

Xu, R. X. 2003, ApJ, 596, L59

Yang, S.-H., Zheng, X.-P., Pi, C.-M., & Yu, Y.-W. 2010, MNRAS, 403, 2007

Yang, S.-H., Pi, C.-M., & Zheng, X.-P. 2011, ApJ, 735, L29

Yu, M., & Xu, R. X. 2011, Astroparticle Physics, 34, 493

Zdunik, J. L. 2002, A&A, 394, 641

Zheng, X., Yang, S., Li, J., & Cai, X. 2002, Physics Letters B, 548, 29

Zheng, X., Yang, S., & Li, J. 2003, ApJ, 585, L135

Zheng, X. P., Kang, M., Liu, X. W., & Yang, S. H. 2005, Phys. Rev. C, 72, 025809

Zhou, E. P., Lu, J. G., Tong, H., & Xu, R. X. 2014, MNRAS, 443, 2705